Earth and Planetary Science Letters 514 (2019) 96–107

Contents lists available at ScienceDirect

Earth and Planetary Science Letters

www.elsevier.com/locate/epsl

Halogens in Atlantis Bank gabbros, SW Indian Ridge: Implications for styles of seafloor alteration

Mark A. Kendrick

Research School of Earth Sciences, Australian National University, Acton, ACT 2601, Australia

ARTICLE INFO

Article history:
Received 28 September 2018
Received in revised form 24 February 2019
Accepted 26 February 2019
Available online 20 March 2019
Editor: M. Bickle

Keywords:
fluorine
chlorine
bromine
iodine
IODP
Expedition-360

ABSTRACT

The processes controlling halogen (F, Cl, Br, I) abundances in gabbroic ocean crust recovered from the 809-m deep Hole U1473A drilled on the Atlantis Bank during International Ocean Discovery Program (IODP) Expedition 360 were investigated. The aims were to provide new constraints on hydrothermal alteration and the abundances of halogens potentially transported to subduction zones in oceanic crust produced on a slow spreading ridge.

Halogens in 51 gabbros and felsic veins have concentrations of ~20-260 ppm F, 15-840 ppm Cl, 44-1230 ppb Br and 1-2490 ppb I. On average the gabbros retain a melt-derived magmatic F component of 58 ± 26% but are dominated by ~96% hydrothermal Cl, Br, I and H_2O. The abundances of hydrothermal Cl, Br and I are consistent with alteration at a seawater/rock ratio of <1. However, hydrothermal F is more enriched than expected and some amphiboles have high F/Cl ratios of 10-30 that provide evidence for the minor additional involvement of F-rich magmatic fluids. The abundant late-stage felsic veins that transect the gabbros and account for 1.5 vol.% of Hole U1473A lithologies are suggested as the most likely source of F-rich magmatic fluids.

Downhole variations show F, Cl, Br and H_2O are most abundant in amphibole- and clay-rich alteration zones at the top of the hole. The highest I concentrations of 1-2.5 ppm delineate an oxidised CO_2-rich alteration zone in which seawater iodate was incorporated into carbonate and Fe-oxyhydroxide alteration. The role of iodate, which is more reactive than other halides, in generating I-rich alteration can be distinguished from alteration by I-rich sedimentary pore waters because the oxidised alteration is characterised by high I/Cl together with low Br/Cl, whereas organic matter in pore waters is enriched in both Br/Cl and I/Cl.

The halogens have inferred compatibilities of $F^- > IO_3^- > OH^- > Cl^- \geq Br^- \sim \geq I^-$ in the investigated alteration assemblage. EPMA and SHRIMP analyses indicate amphibole contains 1000-3000 ppm Cl in amphibolite facies alteration at the top of the Hole. Amphibole, chlorite and talc in greenschist facies alteration have much lower concentrations, typically in the range of 20-800 ppm Cl (median ~100 ppm Cl), and F/Cl ratios of <4. In comparison, low temperature limonite ($FeOOH.nH_2O$) has 160-8500 ppm Cl (median ~840 ppm Cl). Amphibole is the dominant host of Cl and F in amphibolite facies alteration, but chlorite and limonite are important at lower grades. The samples have fairly constant Br/Cl ratios suggesting that Br excluded from the amphibole lattice is retained in minerals such as chlorite and/or non-structural sites. High I concentrations of 10's of ppm are inferred for some carbonate and limonite. Overall amphibole is a less dominant host of halogens than has been suggested previously, which has important implications for the eventual release and availability of halogens during subduction zone metamorphism.

1. Introduction

The alteration of the oceanic crust occurs over a range of temperatures extending from maxima of several hundred degrees in newly formed crust to minima of a few degrees in seafloor settings (e.g. Vanko and Stakes, 1991; Bach et al., 2001; Alt et al., 2010). The largest cumulative effect of alteration is to hydrate and carbonate the oceanic crust as it is transported toward subduction zones. However, seafloor alteration also moderates the composition of seawater and increases the concentrations of fluid mobile elements in the oceanic crust, meaning it is of major importance to the geochemical cycles of many elements (e.g. Bischoff and Dickson, 1975; Philippot et al., 1998; Bach et al., 2001).

E-mail address: mark.kendrick@anu.edu.au.

https://doi.org/10.1016/j.epsl.2019.02.034

The halogens (F, Cl, Br, I) are of special interest from several perspectives. Fluorine increases the stability of hydrous minerals (e.g. Sajeev et al., 2009). Chlorine is the dominant ligand that enables metal transport in hydrothermal fluids, and iodine and bromine are strongly biophilic (e.g. Kendrick, 2018). In addition, subduction-related melts in arc and backarc settings are variably enriched in halogens and H_2O, providing evidence that slab-derived fluids flux the subarc mantle (Straub and Layne, 2003; Sun et al., 2007; Kendrick et al., 2014), and subduction might also be a significant source of halogens in the deeper mantle (Ito et al., 1983; Kendrick et al., 2017). However despite their importance, the concentration ranges and behaviour of halogens in oceanic crust, and particularly the lower gabbroic oceanic crust, are poorly constrained.

Altered ocean crust is enriched in Cl (Ito et al., 1983), and several studies have shown that amphiboles formed from high salinity fluids during amphibolite facies alteration can locally contain wt.% levels of Cl (e.g. Nehlig and Juteau, 1988; Bideau et al., 1991; Vanko and Stakes, 1991; Kendrick et al., 2015). The difficulty of measuring halogens, has however meant that there have been relatively few studies of halogens in the bulk crust (Sano et al., 2008; Zhang et al., 2017). Furthermore, much of our knowledge about crustal halogen abundances is based on a relatively small number of samples from widely spaced locations (e.g. Barnes and Cisneros, 2012; Chavrit et al., 2016). As a result, the range of possible halogen abundances in the crust is poorly defined, limiting our ability to assess halogen loss during subduction zone metamorphism (Philippot et al., 1998; Pagé et al., 2016).

The current study is the first to characterises all four halogens (F, Cl, Br, I), H_2O and CO_2 in a single representative section of oceanic crust combining bulk rock and *in situ* measurements. The aim is to improve understanding of the alteration processes that control halogen concentrations and relative abundances at the crustal scale. For this purpose samples were selected from the 809-m deep International Ocean Discovery Program (IODP) Hole U1473A on the Atlantis Bank of the SW Indian Ridge. The Atlantis Bank is a representative example of an oceanic core complex exhumed on a slow spreading ridge (Dick et al., 2000) and is one of the few basement areas sampled by a deep drill hole. Oceanic gabbros are exposed on the seafloor at Atlantis Bank providing access to lithologies only formed at depths of >2 km at fast spreading centres. Therefore the investigation complements the only previous detailed studies of halogens (F, Cl, Br) in a long section through the upper and mid-crust recovered from Hole U1256D on the superfast East Pacific Rise (Sano et al., 2008; Zhang et al., 2017).

1.1. Hole U1473A, Atlantis Bank

The Atlantis Bank is an elevated flat topped massif at ~700 m water depth on the north-south trending Atlantis II Transform of the SW Indian Ridge (Fig. S1). The Atlantis Bank has been subject to intense study by dredging, remotely operated vehicles, submersible, seabed drilling and four legs of the IODP and Ocean Drilling Program (ODP) (Dick et al., 2000, 2017). The 25 km^2 summit of the Atlantis Bank is interpreted as a wave cut platform (Dick et al., 2000, 2017). Geological mapping combined with information from: ODP Legs 118 (1987) and 176 (1997), which drilled Hole 735B to 1508-mbsf (Dick et al., 2000); and the engineering Leg 179 (1998), which drilled Hole 1105A to 158-mbsf; show the bank is dominated by gabbros which are predicted to transition into altered mantle lithologies ~2-2.5 km below the seafloor (Dick et al., 2017). The Moho at ~6 km is interpreted as a possible hydration front between serpentinised lithosphere and pristine mantle (Dick et al., 2017). The new drilling at Site 1473 was designed to test this model and the lateral heterogeneity of the Bank with a new deep drill hole (Dick et al., 2017).

Hole U1473A reached a depth of 790-mbsf during Expedition 360 and was remediated and slightly deepened to 809-mbsf during a subsequent transit (Dick et al., 2017). The recovered lithologies share many similarities to Holes U735B and U1105A, but differ with respect to the relative abundance of oxide gabbros, the intensity of crystal plastic deformation and the number of carbonate-veined faults (Dick et al., 2017). The stratigraphy of Hole U1473A is dominated by variably altered and deformed olivine gabbros, which represent the most primitive cumulates recovered (#Mg mostly 66-82). Disseminated oxide gabbros (1-2% oxides) and oxide gabbros (>5% oxides) are more evolved and were probably localised by migration of evolved Fe-rich melts through the cumulate pile. The sequence is cut by four dolerite dykes and numerous felsic veins (diorite to trondhjemite) that account for ~1.5 vol.% of the recovered lithologies and are considered to be the result of continued magmatic differentiation (Fig. S1; Dick et al., 2017).

Zircons separated from felsic veins and oxide gabbros recovered from Hole 735B yield U-Pb ages of 12.2-11.9 Ma that reflect the emplacement age of Atlantis Bank gabbros (Rioux et al., 2016). Thereafter, Ar-Ar biotite ages indicate rapid cooling to <400 °C by ~11.4 Ma and fission track zircon and apatite ages demonstrate slower off axis cooling to ~100 °C by ~7 Ma (John et al., 2004). The Atlantis Bank core complex underwent considerable alteration during exhumation. The uppermost part of the Atlantis Bank drill Holes are characterised by high grade granulite to amphibole facies alteration related to cooling from magmatic temperatures and the infiltration of late-stage magmatic fluids and/or seawater (Stakes et al., 1991; Vanko and Stakes, 1991; Natland and Dick, 2001; Alt and Bach, 2006; Dick et al., 2017). At greater depths the Atlantis Bank gabbros are overprinted by lower grade alteration and cut by numerous carbonate veins that formed at ~10-150 °C and are related to later uplift, exhumation and subsidence (Bach et al., 2001; Alt and Bach, 2006; Dick et al., 2017).

2. Sampling and methods

Fifty-one shipboard geochemistry samples encompassing fresh and altered examples of each major lithology were selected. The samples were as large as possible (up to ~40 cm^3) to be representative of coarse-grained (e.g. 2-20 mm) rocks and the coarsest pegmatitic lithologies were avoided. Outside edges were removed to obtain internal parts of drill core that had never contacted metal surfaces or drilling mud. The samples were ultrasonically washed in distilled water for 3 periods of 15 minutes and dried in a furnace at 110 °C before milling in a tungsten-carbide mill (Macleod et al., 2017).

H_2O and CO_2 were measured in 50 mg sized aliquots of whole rock powder using a Thermo Electron Corporation CHNS analyser (Flash EA 1112 Series) on the ship. The reported CO_2 concentrations represent total carbon (C as well as CO_2) and measurements above ~0.1 wt.% H_2O and CO_2 had repeatability of ~5-10% (Macleod et al., 2017). Major elements were analysed by XRF in 50 mg aliquots using a PANalytical Axios Advanced X-Ray spectrometer at the University of Tasmania.

The halogens were analysed at the Australian National University (ANU). SHRIMP was used to measure F in glasses prepared by melting 100 mg of sample powder together with 300 mg of Li-borate flux (Kendrick et al., 2018). Chlorine, Br and I were measured in vacuum encapsulated sample powders (5-20 mg) by the noble gas method. Concentrations of Cl, Br and I are based on the precise measurement of irradiation-produced $^{39}Ar_K$, $^{38}Ar_{Cl}$, $^{80}Kr_{Br}$, $^{128}Xe_I$, calculated K/Cl, Br/Cl and I/Cl ratios and internal standardisation to the XRF K concentrations (Kendrick, 2012; Kendrick et al., 2013a). These methods have detection limits of ~20 ppm for F in whole rocks, sub-ppm for Cl and sub-ppb for

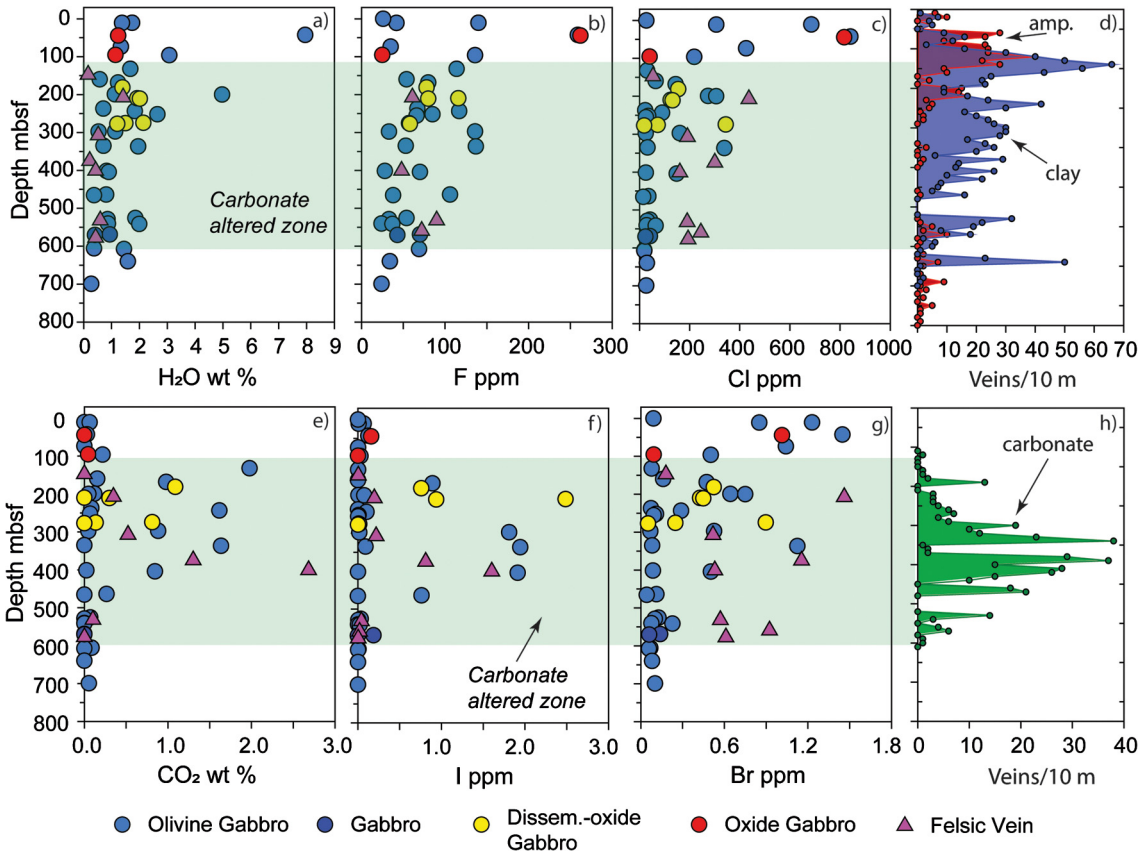

Fig. 1. Depth profiles (mbsf = metres below seafloor) of volatile abundance and vein frequency: a) H_2O in wt.%, b) F in ppm, c) Cl in ppm, d) amphibole and clay mineral vein frequency per 10 metre interval, e) total carbon expressed as CO_2 in wt.%, f) I in ppm, g) Br in ppm and h) carbonate vein frequency per 10 m interval. Vein frequencies were logged by the Shipboard party (Dick et al., 2017). The shaded green band from ~110 mbsf to ~580 mbsf corresponds to high frequencies of carbonate veins as well as high CO_2 and I concentrations. Abbreviation: Dissem.-ox. Gabbro = disseminated oxide gabbro defined as containing 1-2 vol.% oxide minerals. Oxide Gabbro is defined as containing >5 vol.% oxide minerals (Dick et al., 2017). (For interpretation of the colours in the figure(s), the reader is referred to the web version of this article.)

Br and I and precision and accuracy of 2-15% (see Electronic Supplement for details).

Thin sections of whole rocks with variable Cl and I concentrations, and additional samples of characteristic alteration, were investigated by optical microscopy, SEM, SHRIMP and the JEOL 8530F plus electron microprobe at the ANU. Three electron probe microanalysis (EPMA) sessions used currents of 10 nA for silicates and apatite and 4 nA for carbonate. The beam was defocussed to a spot size of 10 µm for apatite and carbonate and 5 µm for silicates. Detection limits were ~60 ppm Cl and either 400 ppm F in Fe-free minerals (session 1; LDE1 crystal) or 150-250 ppm F (sessions 2-3; TAP crystal). SHRIMP with a 30 µm spot size has ppm-level detection limits for both F and Cl. The SHRIMP data were carefully cross calibrated with the EPMA data to check for matrix affects and different calibration curves were adopted for i) silicates and carbonates, and ii) iron oxyhydroxides (see Electronic Supplement). Ten samples were analysed by X-ray Diffraction using a PANalytical Empyrean diffractometer at the University of New South Wales. The data were processed by High Score Plus Software and combined with chemical data to estimate modal mineralogy (see Electronic Supplement).

3. Results

3.1. Whole rock analyses

Representative whole rock data for halogens, H_2O, CO_2 and major elements in each major lithology are summarised in Table 1 and the full dataset for all 51 samples investigated are given in Table S1. The whole rock concentrations range from 0.22 to 8.0 wt.% H_2O, <0.05 to 2.7 wt.% CO_2, <20 to 262 ppm F, 19 to 840 ppm Cl, 44 to 1240 ppb Br and 1 to 2490 ppb I (Fig. 1). The volatile concentrations are controlled by secondary alteration with modal abundance ranging from <3% to ~90% (Table S1), and are not strongly influenced by the samples igneous classification (Fig. 1), which follows previous IODP expeditions: olivine gabbro (>5% olivine), gabbro (<5% olivine), disseminated-oxide gabbro (1-2% oxide), oxide gabbro (>5% oxide) and felsic veins (diorite to tronhjemite) (see Dick et al., 2017).

The samples with the highest H_2O, F, Cl and Br concentrations are all from the uppermost part of the Hole, where amphibolite- and later clay-alteration has the highest abundance (Fig. 1). In contrast, the samples with the highest CO_2 and I concentrations are at depths of between ~100 and ~400 mbsf where carbonate veins have the highest frequency (Fig. 1). Five out of the 51 samples investigated have ppm-level iodine concentrations, which are more typical of organic-rich sediments than igneous rocks (Price and Calvert, 1973; Kendrick, 2018), but are lower than the maximum of 44 ppm I reported for serpentinites (John et al., 2011; Kendrick et al., 2013b).

3.2. Optical microscopy and SEM

The gabbros with the lowest halogen concentrations are dominated by primary minerals (plagioclase, pyroxene and olivine), but minor (e.g. <3%) amphibole and other alteration minerals are always present (e.g. Fig. 2a). In the more strongly altered samples (up to 90%; Table S1), olivine is replaced by various secondary minerals. In some cases chlorite- and talc-rich coronas transition into cores of fine grained iron-oxyhydroxides intergrown with car-

Table 1
Representative whole rock chemical data for Hole U1473A lithologies, Atlantis Bank.

	Oliv. Gabbro	Oliv. Gabbro	Oliv. Gabbro	Oliv. Gabbro	Gabbro	Dissem. Ox. Gabbro	Dissem. Ox. Gabbro	Oxide Gabbro	Felsic Vein	Felsic Vein
Drill core	6R1	37R3	51R4	79R5	63R1	21R1	31R2	11R4	16R6	44R1
U1473A-	98/102	114/118	11/17	70/76	108/112	96/99	117/122	75/78	130/134	10/11
SiO_2	50.1	49.0	51.7	51.2	52.1	50.7	50.3	47.7	58.5	76.0
TiO_2	0.20	0.37	0.34	0.37	0.35	0.88	0.58	2.88	0.09	0.16
Al_2O_3	20.3	18.8	18.6	16.9	18.7	16.3	15.3	12.6	25.3	12.9
Fe_2O_3	7.58	8.46	5.34	5.0	4.54	8.61	9.06	14.4	0.61	0.77
MnO	0.19	0.14	0.10	0.10	0.10	0.16	0.15	0.22	0.01	0.12
MgO	10.9	5.30	7.31	9.11	7.08	5.97	9.59	7.56	0.29	0.85
CaO	9.1	13.9	13.7	14.7	13.8	12.9	12.0	11.4	7.6	4.8
Na_2O	1.37	3.58	3.20	2.52	3.22	3.72	2.71	2.83	7.29	3.27
K_2O	0.260	0.078	0.056	0.030	0.074	0.128	0.071	0.064	0.146	0.110
P_2O_5	bd	0.09	0.02	0.01	0.01	0.02	0.02	bd	0.01	n.d.
SrO	0.01	0.03	0.02	0.02	0.02	0.02	0.02	0.02	0.04	0.01
Cr_2O_3	0.18	0.01	0.02	0.10	0.03	0.01	0.02	0.03	bd	bd
NiO	0.06	0.01	0.01	0.01	0.01	bd	0.02	bd	bd	bd
Total	**100.2**	**99.7**	**100.4**	**100.0**	**100.1**	**99.5**	**99.9**	**99.8**	**99.9**	**99.0**
#Mg	74.0	55.4	73.1	78.3	75.5	57.9	67.7	50.9	48.0	68.6
H_2O wt.%	8.0	2.0	0.81	0.27	0.94	1.4	1.2	1.1	0.16	0.43
CO_2 wt.%	0.03	1.6	0.27	0.05	0.00	1.1	0.00	0.05	0.00	2.7
F ppm	260	140	110	24	70	78	58	25	<20	48
Cl ppm	840 ± 90	340 ± 30	36	27 ± 4	42 ± 13	155 ± 3	19 ± 3	40.2 ± 0.1	54	160
Br ppb	1450 ± 90	1130 ± 50	110	102.1 ± 0.2	140 ± 50	520 ± 30	53 ± 22	94 ± 16	180	530
I ppb	130 ± 50	1940 ± 140	760	1.8 ± 1.0	190 ± 40	760 ± 80	2.0 ± 0.5	3.0 ± 0.2	6	1600

The full dataset for all 51 samples is available in Table S1 of the Electronic Supplement. Uncertainties given for Cl, Br and I in selected samples are the standard deviations of duplicate measurements. bd = below detection.

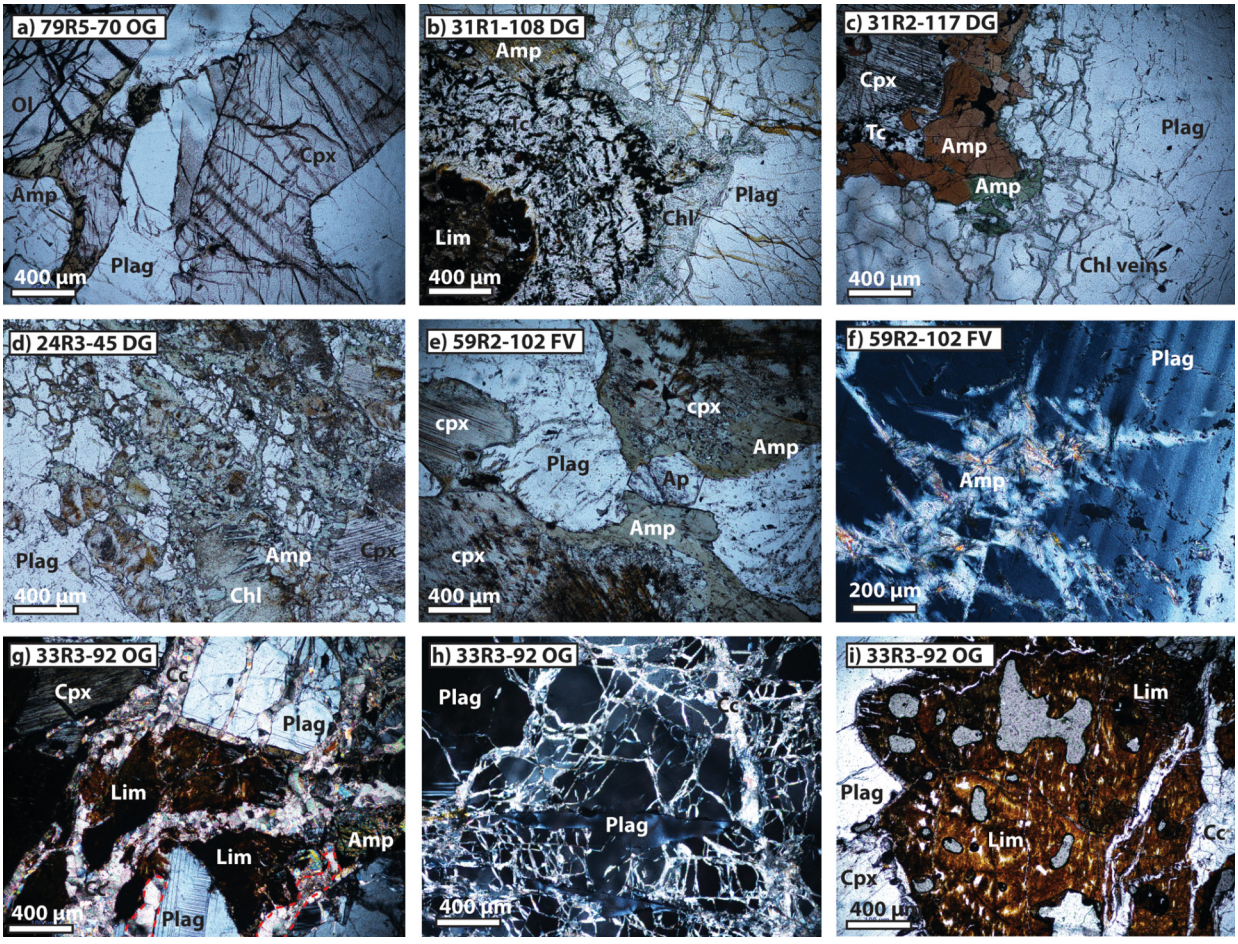

Fig. 2. Transmitted light photomicrographs of representative lithologies from IODP Hole U1473A. a) A largely unaltered olivine gabbro with brownish amphibole of possible magmatic origin. b) Pseudomorphed olivine with a corona of chlorite and talc and a limonite core. Chlorite veins in the outer zone penetrate plagioclase. c) Brown and green amphibole replacing clinopyroxene. Chlorite veinlets in plagioclase. d) Veinlets of chlorite and with acicular green amphibole needles growing from the wall and replacing clinopyroxene. e) Apatite in a felsic vein with clinopyroxene being replaced by green amphibole. f) Fine grained acicular amphibole rosettes replacing plagioclase, x-polars. g) Carbonate veins cutting reddish limonite, plagioclase and partly amphibolitised clinopyroxene, x-polars. h) Carbonate microveinlets in plagioclase, x-polars. i) Reddish limonite cut by carbonate veins.

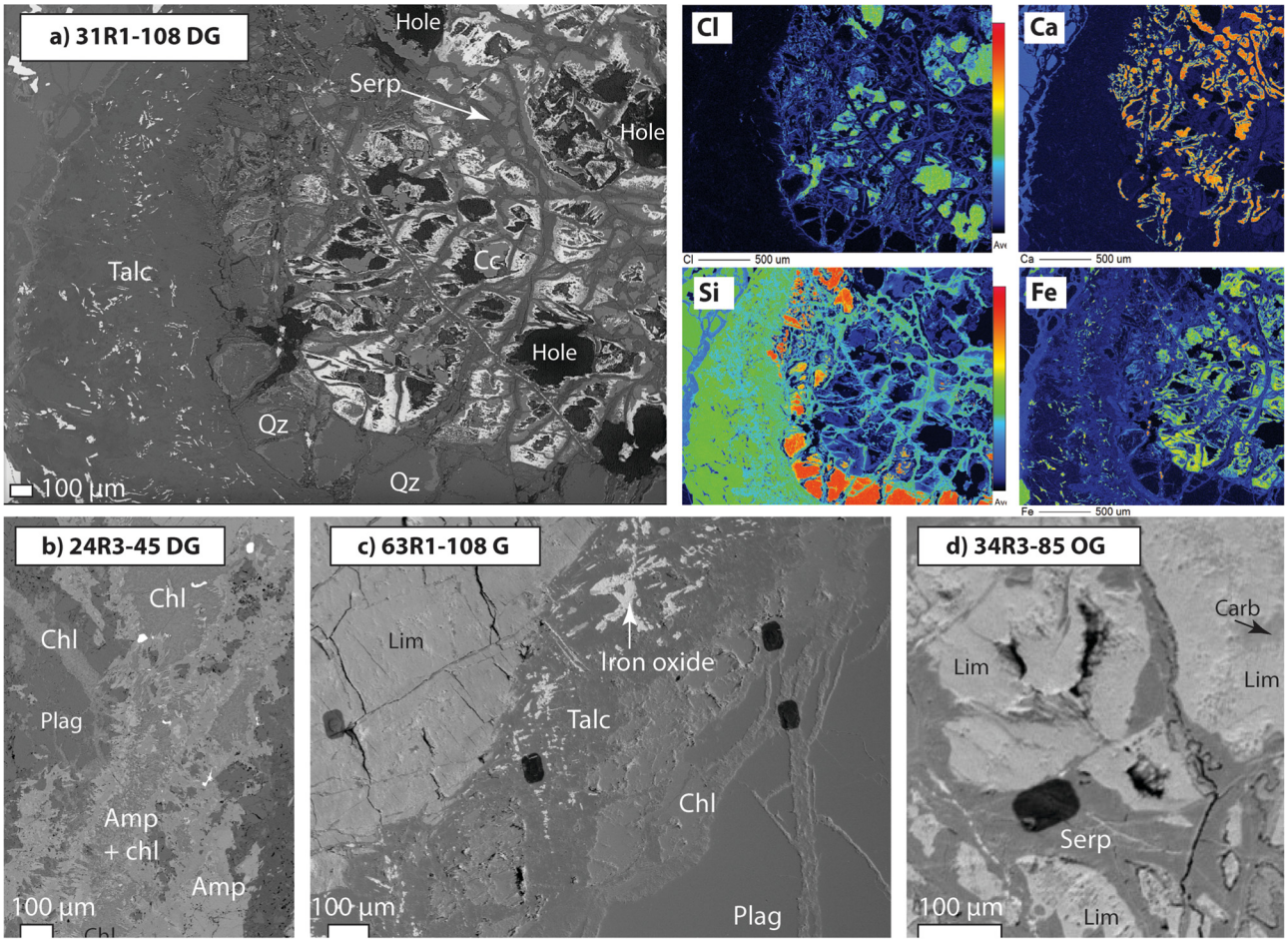

Fig. 3. Backscattered electron images and element maps of characteristic alteration styles from IODP Hole U1473A. a) An olivine pseudomorph in sample 31R1-108 replaced by a mesh of serpentine veins, carbonate, quartz and limonite (see Fig. 2b). Cl is hosted predominantly by the serpentine veins and limonite (but note that the highest intensity areas correspond with holes in the slide: the glue contain Cl but not F). The pseudomorph has a corona of talc and chlorite with ~100 ppm Cl. Areas of quartz, carbonate and limonite are easily identifiable as high intensity areas in the Si, Ca and Fe maps, respectively. b) A chlorite-green amphibole vein in 24R3-45. The amphibole pictured here and Fig. 2d is characterised by high F/Cl. c) Limonite varies from massive in this sample where it has a talc and chlorite alteration halo to highly veined in Figs. 3a and d) where the limonite is intimately intergrown with carbonate. Circular SHRIMP spots (diam = 30 µm) inside rectangular raster areas from which the gold coat has been removed are visible in parts Figs. 3c and d.

bonate (Fig. 2b and 3a), classified here as limonite but termed iddingsite in Hole 735B (Bach et al., 2001). Limonite replaces orthopyroxene as well as olivine and is commonly associated with carbonate and cut by serpentine veinlets (Fig. 3a, d).

Brown amphibole has a coarse grain size in amphibolite facies amphibole-plagioclase veins toward the top of the hole and fine grained patches of brown amphibole are present as lamellae and early alteration of pyroxene in many samples. Brown and green amphibole also replace pyroxene (Figs. 2c, e), and fine grained acicular green and colourless amphiboles occur fringing minerals and closely associated with chlorite and talc (Fig. 2d, f).

Late carbonate veins transect the rocks and cut the limonite (Figs. 2g-i). Clay is a very minor phase in all but one of the samples investigated (6R1-98) where kaolinite replaces plagioclase, but clay is probably also intermixed with the limonite (Deer et al., 1992), which was sometimes logged as red/brown clay during Expedition 360 (Dick et al., 2017). Abundant accessory minerals including zircon, apatite, titanite and monazite are present in the felsic veins (Fig. 2e).

3.3. Electron microprobe and SHRIMP F and Cl data

EPMA and SHRIMP F and Cl measurements on secondary minerals in 19 samples are summarised here and reported fully in the Electronic Supplement. The minimum concentrations measured by SHRIMP were 3-9 ppm F and 5-50 ppm Cl in secondary plagioclase (n = 6). In comparison impure secondary pyroxenes (n = 19), which are often cut by micron scale lamellae and amphibole replacement, gave concentrations of 4-207 ppm F and 12-231 ppm Cl with medians of 30^{+31}_{-6} ppm Cl and 60^{+26}_{-22} ppm F (Table S2).

Brown hornblende in the amphibole-plagioclase veins at the top of the Hole (11R3-13, -118 and 15R2-20) and sample 6R1-98 have 1000-3000 ppm Cl, <100-540 ppm F with typical F/Cl ratios of <0.5 (Fig. 4c, d) similar to Hole 735B lithologies (Fig. 4; Vanko and Stakes, 1991). Epidote in vein 11R3-118 contains ~400 ppm Cl (Fig. 4b). At depths of greater than 140-mbsf, brown and green replacement amphiboles (hornblende and actinolite) have concentrations of 34-800 ppm Cl and 5-300 ppm F, with medians of 108^{+46}_{-43} ppm Cl (n = 75), 116^{+9}_{-32} ppm F (n = 25) and F/Cl of $0.5^{+0.8}_{-0.3}$ (n = 25) that are considered representative of greenschist facies alteration (Fig. 4). A distinctive generation of green hornblende adjacent to chlorite veins in 24R3-45 (Figs. 2d and 3b) and brown amphibole lamellae replacing pyroxene in 33R3-92 have much higher F concentrations of ~600-3200 ppm F and F/Cl ratios of 6-30 (Fig. 4c, d; Tables S2 and S3).

The kaolinite replacing plagioclase (and Cl-rich amphibole) in 6R1-98 in the upper part of the hole has 170-1350 ppm F and 600-2600 ppm Cl (Fig. 4). Mg-Fe chlorite (dominantly pycnochlorite) associated with green amphibole has 22-680 ppm Cl, 21-800

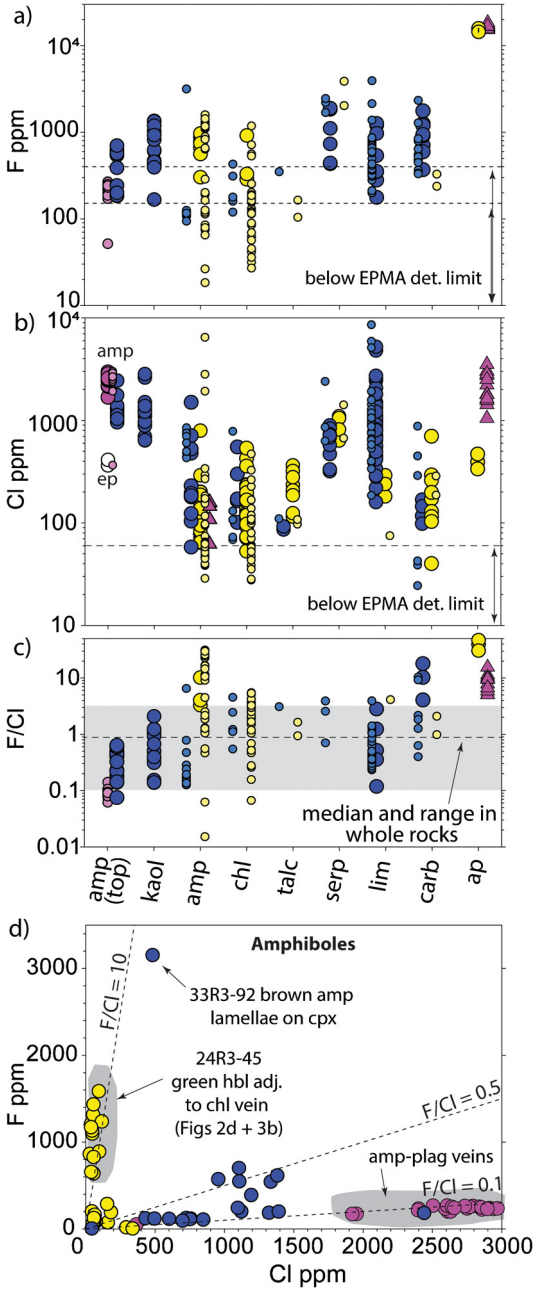

Fig. 4. Mineral concentrations of a) F, b) Cl and c) F/Cl measured by EPMA (large symbols) and SHRIMP (small symbols); and d) F and Cl data for amphiboles. Note that the EPMA detection limits shown varied between sessions (see methods). Legend is as Fig. 1 except amphibole in parts a, b and c is split into 'amp (top)' from the upper 140 m of the Hole, which includes amphibole-plagioclase veins (pink) and amphibole from below 140 mbsf.

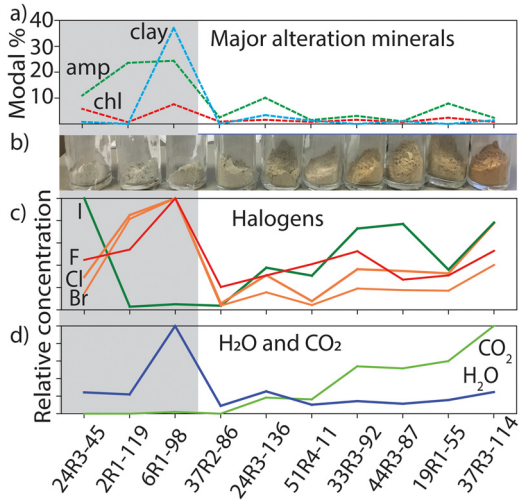

Fig. 5. Modal mineralogy of I- and Cl-rich gabbros. a) Modal abundance of major alteration phases determined via XRD (Electronic Supplement). b) The sample powders organised in order of increasing red colouration, which is a proxy for limonite. c) Relative concentrations of halogens, and d) relative concentrations of H_2O and CO_2. F, Cl and Br have the highest abundance in amphibole rich samples (grey area). H_2O has a high abundance in the clay-rich sample (6R1-98). CO_2 increases with red colouration reflecting the close relationship between limonite and carbonate alteration (see Figs. 3a and d). The highest halogen concentration in the 7 low amphibole samples (white area) occur in the red-coloured limonite rich samples.

ppm F and F/Cl ratios of 0.5-5, with median values of 112^{+27}_{-19} ppm Cl (n = 72), 122^{+51}_{-8} ppm F and F/Cl of 2.1 ± 0.9 (n = 33) (Fig. 4). However, intermixed chlorite and acicular amphiboles in 24R3-45 have locally elevated concentrations of 1000-6000 ppm Cl (n = 4). Limited talc analyses indicate concentration ranges of <60 to 360 ppm Cl with a median of 115^{+92}_{-23} ppm Cl (n = 17); 84-350 ppm F and F/Cl of 1.0-3.4 (n = 4; Fig. 4).

The limonite (~59-66 wt.% FeO ± MnO, ~0.5-4 wt.% Al_2O_3, ~6-14 wt.% SiO_2, ~0.3-1.1 wt.% P_2O_5 with totals of ~80 wt.%) is an intimate mixture of poorly crystalline iron-oxides with variable adsorbed water ($FeOOH.nH_2O$), colloidal silica, phosphates and clays (Deer et al., 1992). The limonite has extremely variable halogen contents of 160-8500 ppm Cl and 200-3900 ppm F, with medians of 849^{+140}_{-74} ppm Cl (n = 90) and 559^{+230}_{-180} ppm F (n =42) (Figs. 4a and 5a), that are similar to what has been reported for Fe-oxyhydroxides previously (Ito and Anderson, 1983; Seyfried et al., 1986). Serpentine veinlets transecting the limonite have 500-2000 ppm Cl, up to 3130 ppm F and F/Cl ratios of 0.7-3.8 (n = 19). Carbonate with median concentrations of 200^{+90}_{-80} ppm Cl (range = 39-875; n = 19) and 570^{+370}_{-180} ppm F (range = 240-1765; n = 11) is present in veinlets and intergrown with the limonite. Calcite dominates, but siderite and dolomite are also present. The late calcite veins (Fig. 2g-i) have up to 3.7 wt.% MgO, <60-170 ppm Cl and 300-1280 ppm F (n = 21). The maximum EPMA and SHRIMP F concentrations in carbonate (1200-1800 ppm) are similar to the maxima of ~1500 ppm F reported for marine carbonates, which typically contain very little Cl (e.g. Opdyke et al., 1993; Kendrick, 2018).

The apatites in the felsic vein 59R5-102 and disseminated-oxide gabbro 24R3-45 have concentrations of 1.4-1.9 wt.% F and 390-3500 ppm Cl (Fig. 4) that are fairly uniform and typical of magmatic apatite. The individual minerals analysed have extremely variable F/Cl of 0.01 to 47 (Fig. 4). However, the median F/Cl of all 188 SHRIMP analyses ($0.98^{+0.17}_{-0.34}$) is indistinguishable from the median ($0.9^{+0.3}_{-0.2}$) obtained for whole rocks (Fig. 4). The whole rock halogen concentrations depend on both the degree of alteration (ranging <3% to 90%; Table S1) and the halogen content of the alteration minerals, which is highest in amphibolite facies samples at the top of the Hole.

3.4. XRD of chlorine- and iodine-rich gabbros

Modal abundances of major alteration minerals (amphibole, chlorite and clay) in ten I- or Cl-rich gabbros obtained from combined XRD spectra and bulk chemistry are summarised in Fig. 5a. Trace amounts (e.g. <3%) of talc, carbonate, clay, mica and serpentine were detected in several samples (Electronic Supplement). The poorly crystalline nature of limonite (Deer et al., 1992) meant that it was difficult to quantify, but a minimum modal abundance of

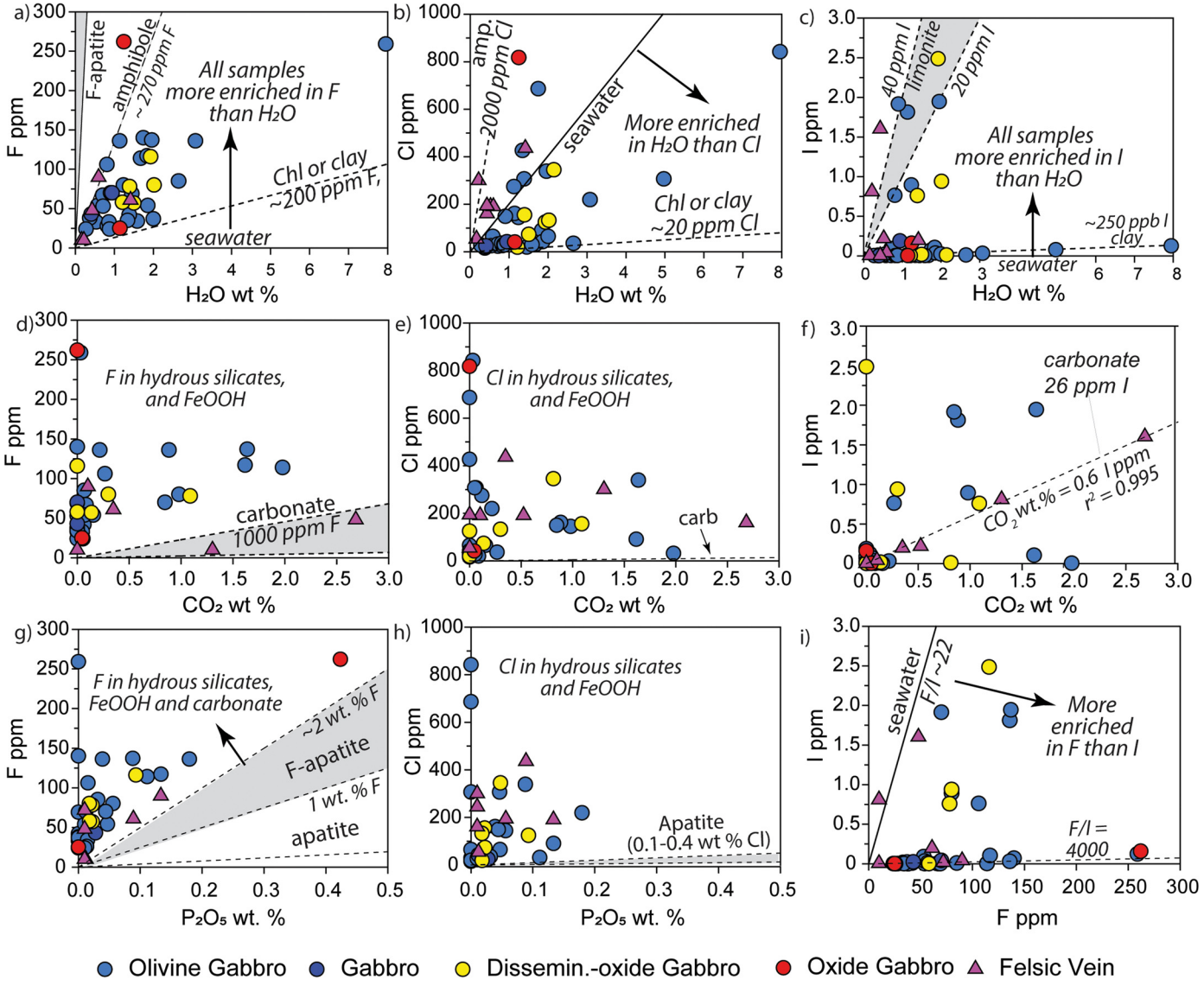

Fig. 6. The halogen (F, Cl, I), H_2O, CO_2 and P_2O_5 content of gabbros and felsic veins from Hole U1473A. a) F versus H_2O, b) Cl versus H_2O, c) I versus H_2O, d) F versus CO_2, e) Cl versus CO_2, f) I versus CO_2, g) F versus P_2O_5, h) Cl versus P_2O_5 and i) I versus F. The slopes represent the calculated compositions of seawater and various important or potentially important mineral phases.

3.5% was obtained for 19R1-55 and the samples red colouration, suggests a slightly higher abundance in 37R3-114 (Fig. 5b).

The most Cl-rich samples (6R1-98, 840 ppm Cl; 2R1-119, 690 ppm Cl) contain ~24% amphibole and 0-8% chlorite, consistent with average concentrations of more than ~2000 ppm Cl in the amphibole and chlorite of these samples (Figs. 4 and 5; Table 1). Sample 6R1-98 with an unusually high concentration of 8 wt.% H_2O is the only sample investigated with significant clay replacement of plagioclase (~37% kaolinite; Fig. 5; Electronic Supplement). The samples red colouration increases with CO_2 concentration to a maximum of 1.6 wt.% CO_2 in 37R3-114 (Fig. 5; Table 1), which is consistent with the observed close relationship between red coloured limonite and carbonate (Fig. 3d). In samples with low modal amphibole abundances (white area in Fig. 5), halogens increase systematically with red colouration to maxima of 340 ppm Cl and 1.9 ppm I in 37R3-114 (Fig. 5; Table 1), consistent with limonite as a major halogen host (Figs. 4 and 5). However, sample 24R3-45 with negligible limonite has the highest measured I concentration of 2.5 ppm (Fig. 5).

4. Discussion

4.1. Halogen mineral hosts and relative compatibility

Plots of F, Cl and I against H_2O, CO_2 and P_2O_5, can be used together with the in situ F and Cl, and XRD data to make inferences about the dominant mineral hosts of halogens (Fig. 6). Bromine is not included in Fig. 6 because it is strongly correlated with Cl (Fig. 7), meaning that plots with either Br or Cl yield similar information.

The majority of whole rock samples have F/H_2O of between 0.014, equivalent to an amphibole with ~270 ppm F, and 0.0013 equivalent to a H_2O-rich mineral such as chlorite, limonite or clay with ~200 ppm F (Fig. 6a). Two felsic veins have F/CO_2 within the range of carbonate (Fig. 6d), but none of the samples have F/P_2O_5 completely within the F-apatite range (Fig. 6g). Apatite is estimated to host 55-62% of the total F in the felsic veins and oxide gabbro that plot closest to the F-apatite field (Fig. 6g). In contrast, apatite is a negligible host of F in P-poor samples and on aver-

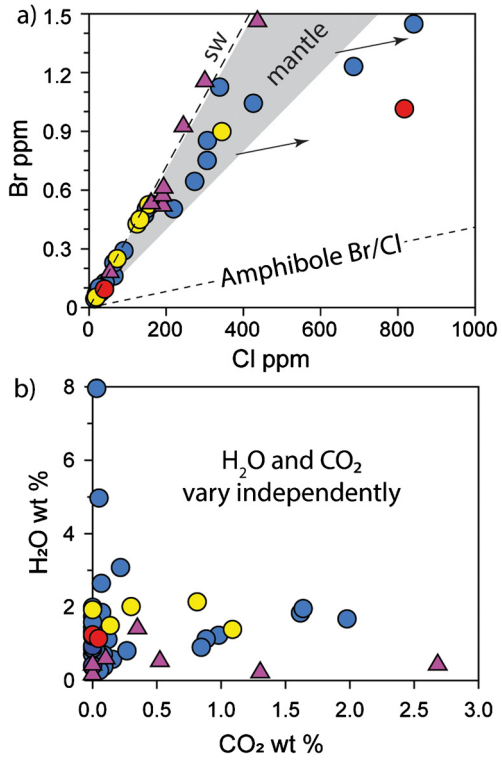

Fig. 7. Plots of a) Br versus Cl and b) H_2O versus CO_2. Legend as in Fig. 6. Slopes representative of seawater (SW), pristine MORB glasses (grey field) and typical amphibole Br/Cl ratios are shown for reference (Kendrick et al., 2017, 2015). The arrows in part a represent vectors for amphibole alteration. The data indicate Br excluded from amphibole is incorporated into other minerals, such as chlorite, talc, limonite or fluid inclusions and halogens could have been derived from either seawater or magmatic fluids.

age hosts only 10-20% of the total F (Table S1), indicating hydrous silicates and limonite as the dominant F hosts.

The majority of whole rocks have Cl/H_2O ratios intermediate of 0.1, equivalent to amphibole with ~2000 ppm Cl, and a value of 0.0003, equivalent to a H_2O-rich mineral like chlorite or clay with ~20 ppm Cl (Fig. 6b). Amphibole is a major Cl host in amphibolite facies rocks where amphibole is abundant and has a high Cl content (Fig. 5). The low Br/Cl ratios of samples with >600 ppm Cl are explained because Br is preferentially excluded from amphibole relative to Cl (Fig. 7a; Kendrick et al., 2015). In contrast, the similar concentrations of Cl in amphibole and chlorite (Fig. 4) and their relative abundances (e.g. Fig. 5) imply that chlorite is an important host of halogens in some samples. Furthermore, the narrow range of Br/Cl ratios in samples with <600 ppm Cl (Fig. 7a), implies that Br excluded from amphibole must be taken up by minerals like chlorite or trapped in non-structural sites: halogens trapped along grain boundaries or originally present in melt and fluid inclusions, which can be abundant in plagioclase and are present in most minerals, will be present in our unwashed sample powders. Apatite and carbonate, are indicated as minor Cl hosts (e.g. <2% of total Cl). Limonite is an important Cl host in low grade samples (Figs. 4 and 5).

The strong correlation of I and CO_2 in the felsic veins (r^2 = 0.995; Fig. 6f) might be explained because seawater iodate can substitute for carbonate (iodine is the only halogen that exists in an oxidised form in seawater; Claret et al., 2010; Lu et al., 2010). If iodine is hosted by the carbonate veinlets observed in the felsic veins, the best fit regression in Fig. 6f implies an average of ~26 ppm I in carbonate. This is ten times higher than the ~2 ppm incorporated into calcite experimentally (Claret et al., 2010; Lu et al., 2010), but given that lauterite [$Ca(IO_3)_2$] is a known phase, high concentrations maybe feasible given the involvement of sufficiently I-rich fluids and/or favourable pressure-temperature conditions. The lack of a correlation between CO_2 and I in gabbros (Fig. 6f), might be explained because I is present in limonite as well as carbonate in the gabbros. Limonite formed after olivine or pyroxene is a favoured I-host because: i) many of the samples with strong red colouration are I-rich (Fig. 5), and ii) seafloor Mn/Fe oxides contain 100-2500 ppm I (Baturin, 1988). If correct, the modal abundance of limonite (<4%) and sample I/H_2O ratios implies limonite alteration could contain ~20-40 ppm I (Fig. 6c), some of which might be hosted by carbonate or serpentine veinlets within the limonite (e.g. Fig. 3a, d). The I concentration inferred for most limonite is much lower than reported for seafloor Mn/Fe oxides (100-2500 ppm I; Baturin, 1988), meaning that scarce I-rich limonite in 24R3-45 could potentially still account for this samples strong I enrichment (cf. Fig. 5). Alternatively, I could be hosted by an unidentified mineral phase or unusual fluid inclusions in this sample.

The samples F/H_2O, Cl/H_2O and I/H_2O ratios (Fig. 6a, b and c) show that compared with seawater, the altered gabbros have strong enrichments in F and I relative to H_2O, but the majority are enriched in H_2O relative to Cl (and Br). The samples F/I ratios demonstrates that the altered gabbros are more enriched in F than I, but two carbonate-altered felsic veins preserve near seawater F/I (Fig. 6i). If the halogens were derived mostly from seawater, these observations imply relative compatibilities in the alteration minerals of $F > I > H_2O > Cl \geq Br$. The coherent behaviour of Cl and Br in the majority of samples implies very similar compatibilities during alteration; however, Br is less compatible than Cl in amphibole-rich samples (Fig. 7; Kendrick et al., 2015).

4.2. Sources of halogens and amphiboles

Most Atlantis Bank lithologies have Br/Cl within the compositional range of pristine ocean crust and the mantle (Fig. 7; defined by MORB glasses; Kendrick et al., 2017) allowing the possibility that a significant portion of the halogens could have been derived from either late-stage magmatic fluids (with mantle like Br/Cl) or remobilised from elsewhere within the oceanic crust (Kendrick, 2018).

The brown hornblende in the amphibole-plagioclase veins at the top of the hole and amphibole replacement in samples 6R1-98 and 2R1-119 have high Cl concentrations and low F/Cl ratios (Figs. 4d and 5) typical of amphiboles grown from high salinity seawater-derived fluids. Similar Cl-rich amphibole veins were reported at the top of Hole 735B, where fluid inclusions provide evidence for the passage of variably saline (e.g. 5-25 wt.%) seawater-derived fluids (Vanko and Stakes, 1991).

The majority of the brown and green replacement amphiboles with median Cl concentrations of ~100 ppm, are characterised by low F/Cl ratios of <1 (Fig. 4d) that are typical of greenschist facies alteration by low salinity seawater-derived fluids (Vanko and Stakes, 1991). Small brown amphibole lamellae and replacement were difficult to locate with the SHRIMP optics, but the majority of alteration lamellae analysed together with secondary pyroxene have F/Cl of <1 that are consistent with alteration by seawater-derived fluids.

In contrast, the presence of F-rich brown amphibole lamellae in sample 33R3-92 and F-rich green vein hornblende associated with chlorite in 24R3-45 provide evidence for late-stage magmatic fluids (Figs. 2d, 3b and 4d). Hydrothermal amphiboles with ~600-3000 ppm F and F/Cl of 10-30 are unlikely to form from seawater-derived hydrothermal fluids with F/Cl of <0.0001 (Kendrick, 2018). Instead they provide evidence for the passage of late-stage magmatic fluids exsolved from silicic magmas, which can have much higher F contents (Webster, 1990). The locally elevated concentrations of 1000-6000 ppm Cl in chlorite-amphibole veins adjacent

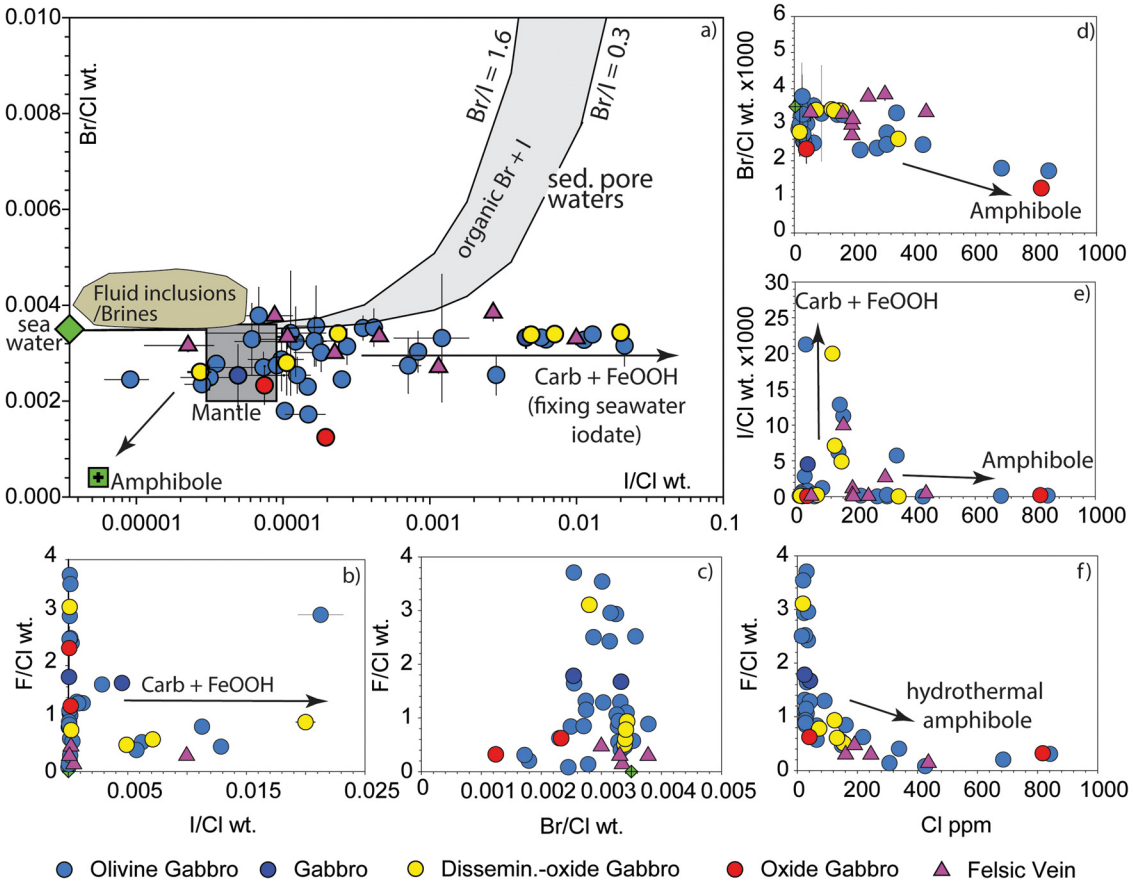

Fig. 8. Halogen abundance ratios and Cl concentrations of Hole U1473A lithologies. a) Br/Cl versus I/Cl plot showing the compositional ranges of seawater, sedimentary pore waters, the mantle (based on MORB and OIB glasses; Kendrick et al., 2017), amphibole and high salinity fluid inclusions/brines (Kendrick et al., 2015). Additional references are given in Kendrick (2018). b) F/Cl versus I/Cl. c) F/Cl versus Br/Cl. d) Br/Cl versus Cl ppm, e) I/Cl versus Cl ppm and f) F/Cl versus Cl ppm. Seawater-derived iodate is incorporated into carbonate, limonite and other minerals during oxidised alteration. The most Cl-rich samples have fractionated Br/Cl ratios characteristic of amphibole.

to the F-rich amphibole in 24R3-45, favour high salinity fluids demonstrating large fluctuations in the nature of fluids altering this sample.

4.3. Alteration fluid oxidation state

The lithologies recovered from Hole U1473A are variably enriched in I relative to Br and Cl with the data defining a distinctive horizontal trend in Fig. 8. The iodine enrichment can be explained by the redox sensitivity of I, which exists as iodate in seawater (Kendrick, 2018), coupled with the high reactivity of iodate compared with other halides (Claret et al., 2010; Lu et al., 2010). Iodate is readily adsorbed onto various materials including clay minerals, organic matter and ferrous/manganese-oxides (Price and Calvert, 1973; Kendrick, 2018) and it is also incorporated into the lattice of carbonate (Claret et al., 2010; Lu et al., 2010).

The precise analysis of Cl, Br and I enables us to distinguish different causes of I-enrichment. Sedimentary pore waters are enriched in both Br and I by the regeneration of organic matter (Muramatsu et al., 2007) and serpentinites formed by alteration with sedimentary pore waters can be recognised by their elevated Br/Cl and I/Cl ratios that are similar to sediment pore waters (John et al., 2011; Kendrick et al., 2013b). In contrast, high I/Cl together with low (or mantle-like) Br/Cl ratios in this study (Fig. 8) appear to be a characteristic of alteration by low temperature, oxidised (iodate-bearing) fluids.

The lithologies in Hole U1473A record several different styles of overprinting alteration related to the passage of multiple fluid pulses through the crust. Seawater was almost certainly the dominant fluid but distinct pulses of magmatic fluid are recorded by F-rich amphiboles (Fig. 4d) and variations in the fluids oxidation state and salinity are recorded by the degree of I-enrichment (Fig. 1) and amphibole chlorinity (Fig. 4d). The downhole iodine concentration data delimit an oxidative alteration zone that overlaps the interval of maximum carbonate vein intensity (Fig. 1). A similar oxidative alteration zone ascribed to the passage of low temperature relatively unreacted seawater was recognised in Hole 735B (Bach et al., 2001).

4.4. Residual porosity and the degree of halogen enrichment

The original concentrations of halogens in the Atlantis Bank gabbros can be approximated using estimates of inter-cumulus residual melt porosity (e.g. the amount of melt retained between cumulate phases) and the residual melt composition (Natland and Dick, 2001). The average residual porosity can be estimated from the gabbros median P_2O_5 concentration of $0.015^{+0.008}_{-0.002}$ wt.%, because P_2O_5 is excluded from cumulate minerals and is present in accessory phases like apatite that crystallise from residual melts (Natland and Dick, 2001). The calculated residual porosity is sensitive to the assumed residual melt composition: an upper limit of 11 ± 5% is estimated from melts with 0.14 wt.% P_2O_5 similar to primitive SW Indian Ridge MORB, and a lower limit of 4 ± 2% is estimated from evolved melts with 0.4 wt.% P_2O_5. These ranges are similar to estimates for residual porosity in Hole 735B gabbros based on Zr (Natland and Dick, 2001).

Table 2
Average composition of Atlantis Bank Gabbros, Hole U1473A, and related reservoirs.

	F	Cl	Br	I	H_2O
SWIR MORB	170-220 ppm	14-40 ppm	45-110 ppb	1-3 ppb	0.1-0.3 wt.%
Minimum gabbro	~20 ppm	15 ppm	44 ppb	1 ppb	0.27 wt.%
Maximum gabbro	260 ppm	840 ppm	1230 ppb	2490 ppb	8.0 wt.%
Altered gabbro (Mean ± SD)	72 ± 57 ppm	150 ± 210 ppm	370 ± 390 ppb	310 ± 630 ppb	1.6 ± 1.4 wt.%
Altered gabbro (Tukey's Biweight)[a]	64 ± 13 ppm	97 ± 36 ppm	340 ± 120 ppb	8 ± 3 ppb	1.3 ± 0.3 wt.%
Average magmatic component (calculated)	37 ± 15 ppm	4 ± 2 ppm	11 ± 6 ppb	0.24 ± 0.17 ppb	0.04 ± 0.02 wt.%
Proportion of magmatic component (%)	58 ± 26%	4 ± 3%	3 ± 2%	3 ± 2%	3 ± 1%
Average hydrothermal component	27 ± 20 ppm	93 ± 36 ppm	330 ± 120 ppb	8 ± 3 ppb	1.3 ± 0.3 wt.%
Average enrichment factor	1.7 ± 0.8	24 ± 15	31 ± 20	33 ± 27	34 ± 16
Maximum enrichment factor	7	210	110	10,400	210
Seawater	1.3 ppm	19,000 ppm	66,500 ppb	58 ppb	96.5 wt.%
W/R (mass ratio)	62 ± 46	0.01 ± 0.01	0.01 *T*± 0.01	0.4 ± 0.2	0.04 ± 0.01

[a] The Tukey's Biweight is similar to the median. We use it in our calculations because it better represents typical gabbros with skewed (*log-normal*) trace element distributions than the mean. The Tukey's Biweight was calculated using the Isoplot program.

In contrast with P_2O_5, F is significantly accommodated by some cumulate minerals. At ~1250 °C the F partition coefficients $D_{mineral/melt}$ are probably ~0.001 for olivine and ~0.04-0.1 for pyroxenes and plagioclase (Beyer et al., 2012; Dalou et al., 2012; Joachim et al., 2015). Assuming a bulk partition coefficient of 0.03-0.08, primary cumulate phases formed from evolving melts with 170-300 ppm F, overlapping SW Indian Ridge MORB, would contain 5-24 ppm F. Pairing either our upper limit of residual porosity (~11 ± 5%) with primitive SW Indian MORB containing 170-220 ppm F (Kendrick et al., 2017), or our lower estimate of residual porosity (~4 ± 2%) with an evolved melt containing 480-620 ppm F, yields equivalent contributions to bulk rock F concentration of 22 ± 11 ppm. Taking the cumulate phases (5-24 ppm F) and residual melts together, the Atlantis Bank gabbros are therefore estimated to have a median concentration of 37 ± 15 ppm melt-derived magmatic F (Table 2).

The concentration of magmatic Cl, Br, I and H_2O can be estimated in a similar way. Assuming Cl, Br and I have similar bulk partition coefficients of 0.005-0.01 (Beyer et al., 2012; Dalou et al., 2012; Joachim et al., 2015) and formed from melts similar to SW Indian Ridge MORB with 14-50 ppm Cl (Kendrick et al., 2017), cumulate phases would have only 0.1-0.5 ppm Cl. As a result, the residual melts dominate the estimated whole rock concentrations of 4 ± 2 ppm magmatic Cl, 11 ± 6 ppb magmatic Br and 0.24 ± 0.17 ppb magmatic I (Table 2). The residual melts would have contained from 0.1-0.3 wt.% H_2O if they were similar to SW Indian MORB, to ~0.9 wt.% H_2O if they were more evolved, suggesting a contribution of 100-300 ppm magmatic H_2O to bulk rock concentrations. An upper limit of 380 ± 150 ppm magmatic H_2O is obtained by scaling the concentrations of magmatic H_2O and F in SW Indian Ridge MORB and the Atlantis Bank Gabbros, which implicitly assumes these elements have similar compatibilities (Table 2).

The difference between the concentrations of halogens and H_2O measured in the altered gabbros and estimated for pristine gabbros containing only melt-derived magmatic halogens enables the degree of hydrothermal enrichment to be estimated (Table 2). Given that trace element concentrations have skewed (log-normal) distributions we use the Tukey's Biweight of measured values, which is similar to the median and provides a more representative 'average' for the altered gabbros than the mean. On this basis typical alteration-related enrichment factors are estimated as ~2 for F and ~25-35 for Cl, Br, I and H_2O (Table 2). This indicates that more than ~96% of the heavy halogens and H_2O have been introduced by alteration fluids but a melt-derived magmatic component is important for F (Table 2).

The water/rock mass ratios required to introduce the calculated concentrations of hydrothermal halogens from seawater are estimated as <0.5 for the heavy halogens and water, which is broadly consistent with the generally low water/rock ratios proposed for Atlantis Bank alteration previously (Stakes et al., 1991; Vanko and Stakes, 1991; Bach et al., 2001). In contrast, the calculated water/rock ratio of 62 ± 46 for F, shows that the required quantity of hydrothermal F cannot be easily derived from seawater. Together with the presence of F-rich amphiboles (Fig. 4d), this is interpreted as evidence for the involvement of F-rich magmatic fluids exsolved from late-stage felsic veins.

Hydrothermal fluids from the PACMANUS vent field have F concentrations of up to four times seawater that is ascribed to a small magmatic contribution (Reeves et al., 2011). The F content of magmatic fluids exsolved from evolving melts is variable and poorly defined (Webster, 1990); however, if the magmatic fluid had a sufficiently high F/Cl ratio, a very small (e.g. sub % level) contribution could explain the F-enrichment of Atlantis Bank gabbros (Table 2). A magmatic fluid component in Atlantis Bank alteration is also favoured by low δD (c. -60‰) in some rocks and vein hornblendes recovered from Hole 735B (Alt and Bach, 2006).

4.5. Comparison with previous studies and implications

The Atlantis Bank gabbros recovered by Holes U1473A (809-m) and 735B (1508-m) have similar concentration ranges of 15-900 ppm Cl (median ~100 ppm Cl; Table 1; Barnes and Cisneros, 2012) that decrease from maxima associated with amphibolite facies alteration in the upper 200-m of the holes to lower values at depth (Fig. 1). In contrast, lavas, dykes, and the uppermost gabbros recovered from Hole 1256D (1522-m) in the superfast East Pacific Rise have Cl concentrations that are ~2-4 times higher (e.g. 100-1400 ppm Cl, median ~360 ppm Cl) and increase with depth (Sano et al., 2008; Zhang et al., 2017).

The differences are explained by a combination of factors related to the different tectonic settings. Hole 1256D samples a 1.5 km 'intact' section of the East Pacific Rise going through lavas, dykes and into the uppermost gabbros (Expedition 309/312 Scientists, 2006). The intense alteration of these lithologies is explained by proximity to an underlying melt lens that drove vigorous hydrothermal circulation, which is common on fast spreading ridges (Expedition 309/312 Scientists, 2006; Sano et al., 2008; Alt et al., 2010). In contrast, the Atlantis Bank gabbros were exhumed in an oceanic core complex on a slow spreading ridge (Dick et al., 2000). The thickness (and structure) of crust formed on slow and fast spreading ridges is different (Dick et al., 2003). The Atlantis Bank gabbros represent lithologies originally formed at greater depth equivalents than the uppermost gabbros from 1256D (Dick et al., 2000, 2017). However, they have been affected by greenschist and low temperature alteration related to seawa-

ter infiltration during uplift, exhumation and subsidence (Bach et al., 2001). Therefore the Atlantis Bank gabbros record a range of igneous and metamorphic processes typical of 'lower crust' and overprinting styles of alteration typical of 'upper crust' formed on a fast spread ridge.

In combination, it appears that Cl concentrations increase with depth through greenschist to amphibolite facies over depths of >1.5 km to a peak of at least ~1400 ppm in Hole 1256D gabbros, and over an unknown depth to a peak of at least ~900 ppm in Atlantis Bank gabbros (Fig. 1; Sano et al., 2008; Barnes and Cisneros, 2012). The Cl concentrations then decrease to very low background values of 15-50 ppm over a depth of less than ~500-m in Hole U1473A (Fig. 1). However, our data confirm that even in the absence of seawater infiltration, the lower crust is locally altered by (Cl and) F-rich magmatic fluids derived from crystallising felsic veins. In contrast with Cl, the strong I-enrichment of Hole U1473A associated with low temperature carbonate-Fe-oxide alteration reaches a peak between 100 and 450-mbsf (Fig. 1) and is similar to alteration reported at basement depths of <500-m in intact fast spread crust (Alt et al., 2010).

Previous studies have invariably identified amphibole and apatite as dominant halogen hosts in ocean crust (Ito and Anderson, 1983; Ito et al., 1983; Barnes and Cisneros, 2012; Chavrit et al., 2016; Zhang et al., 2017). In contrast, the data from Hole U1473A show a more complex picture. Apatite is a minor reservoir of F and Cl in all but the most evolved felsic veins. The concentrations of Cl in amphiboles are similar to previous studies; 10's to 100's of ppm in greenschist facies alteration and thousands of ppm in amphibolite facies alteration (Nehlig and Juteau, 1988; Bideau et al., 1991; Vanko and Stakes, 1991). Amphibole is therefore confirmed as a major reservoir of halogens in amphibolite facies rocks (Ito et al., 1983), which can have low Br/Cl ratios (Figs. 7 and 8). However, the electron microprobe, SHRIMP, XRD and whole rock data (Figs. 4–6) suggest that chlorite and Fe-oxyhydroxide (with associated carbonate and serpentine) are important F and Cl hosts at lower grades; and limonite and carbonate are probably the dominant I repositories. Abundant clay was present in only one of our samples (6R1-98) and may have inherited high F and Cl concentrations from the amphibole in this sample (Fig. 4). However, the bulk rock data imply that the majority of chlorite or clay probably has much lower Cl concentrations (Fig. 6c), consistent with the low Cl content of clay veins (Magenheim et al., 1995) and palagonite alteration (Kendrick, 2018) reported previously. Previous studies have suggested clay as a major I-host (Chavrit et al., 2016; Kendrick, 2018); however, the current data imply a maximum concentration of ~250 ppb I in clay compared with 10's of ppm in limonite and carbonate (Fig. 6c).

Further data for all hydrous minerals in the oceanic crust from a range of settings are required to improve constraints on the distribution of halogens in altered ocean crust. This is critical because halogens will be released at different stages of the subduction cycle depending on their mineral or fluid inclusion host. Ito and Anderson (1983) regarded iddingsite as a highly soluble ephemeral phase that would be unimportant to deep subduction budgets. Fe-oxyhydroxides do have relatively high solubilities (Seyfried et al., 1986). However, the Cl rich phase associated with limonite in our samples was not removed by preparation of thin sections with water. Furthermore, such phases could be highly significant for subduction budgets; even if they only retain halogens to moderate subduction depths they could contribute halogen-rich fluids with high I/Cl to the forearc, which might be trapped in newly formed phases and lithologies, including forearc serpentinites that are stable to much greater depths (Bostock et al., 2002). It might therefore be significant that subducted components identified in the majority of back arc basins investigated to date either have Br/Cl and I/Cl similar to the mantle, or elevated I/Cl and low Br/Cl ratios (Kendrick et al., 2014), that are more similar to the alteration identified in this study than sedimentary pore waters characterised by elevated Br/Cl and I/Cl ratios (Fig. 8).

5. Summary and conclusions

Atlantis Bank gabbros have strongly variable concentrations of halogens and H_2O. More than ~96% of the total Cl, Br, I and H_2O in the gabbros were introduced by seawater-derived fluids, whereas 58 ± 26% of the F has a magmatic origin from the melt. The concentrations of hydrothermal Cl, Br, I and H_2O in the gabbros indicate an integrated seawater/rock ratio of <1. In contrast, unexpectedly high concentrations of hydrothermal F in whole rocks, and amphiboles with high F/Cl ratios of >10, require a small contribution of (Cl and) F-rich magmatic fluids to the hydrothermal system.

The relative compatibilities of halogens in the investigated alteration assemblage (abundant amphibole, chlorite, limonite, carbonate, with lesser talc, serpentine and minor clay) is $F > I > H_2O > Cl \geq Br$. However, high concentrations of I are characteristic of oxidised alteration (Figs. 1 and 8), so a fuller description of relative compatibility is: $F^- > IO_3^- > OH^- > Cl^- \geq Br^- \sim \geq I^-$.

The Atlantis Bank gabbros contain 2-4 times less halogens than lavas, dykes and gabbros recovered from Hole 1256D on the East Pacific Rise, which reflects differences in the original relative depths of the crustal sections investigated and hydrothermal processes on slow and fast spreading ridges. In addition to amphibole, chlorite and limonite are important Cl and F hosts and carbonate and limonite are suggested as major I repositories (e.g. concentrations of ~20-40 ppm I). Further characterisation of halogen mineral hosts in other seafloor settings is required to improve our understanding of halogen subduction budgets.

Acknowledgements

Dr. M.A. Kendrick was supported by an Australian Research Council Future Fellowship (FT13 0100141). This work would not have been possible without the support of the International Ocean Discovery Program (IODP) and Australia-New Zealand IODP Consortium (ANZIC), which enabled Kendrick's participation in Expedition 360. The IODP provided the samples and ANZIC provided post-cruise funding for this study. ANZIC is supported by the Australian Government through the Australian Research Council's LIEF funding scheme (LE140100047 and LE160100067) and the Australian and New Zealand consortium of Universities and government agencies. Kendrick greatly benefited from discussions with various members of the Expedition 360 Scientific Party both aboard the Joides-Resolution and in post-cruise settings: good hearty shellbacks the lot of them. Kendrick is grateful for the expert technical support of Pete Holden in the ANU SHRIMP laboratory and Xiaodong Zhang in the noble gas laboratory. Saroj Bhattacharyya at the UNSW X-ray Diffraction Laboratory is thanked for the XRD data. The author acknowledges the facilities, and the scientific and technical assistance, of the Australian Microscopy & Microanalysis Research Facility at the Centre of Advanced Microscopy, the Australian National University.

Appendix A. Supplementary material

Supplementary material related to this article can be found online at https://doi.org/10.1016/j.epsl.2019.02.034.

References

Alt, J.C., Bach, W., 2006. Oxygen isotope composition of a section of lower oceanic crust, ODP Hole 735B. Geochem. Geophys. Geosyst. 7.

Alt, J.C., Laverne, C., Coggon, R.M., Teagle, D.A.H., Banerjee, N.R., Morgan, S., Smith-Duque, C.E., Harris, M., Galli, L., 2010. Subsurface structure of a submarine hydrothermal system in ocean crust formed at the East Pacific Rise, ODP/IODP Site 1256. Geochem. Geophys. Geosyst. 11.

Bach, W., et al., 2001. The geochemical consequences of late-stage low-grade alteration of lower ocean crust at the SW Indian Ridge: results from ODP Hole 735B (Leg 176). Geochim. Cosmochim. Acta 65, 3267–3287.

Barnes, J.D., Cisneros, M., 2012. Mineralogical control on the chlorine isotope composition of altered oceanic crust. Chem. Geol. 326–327, 51–60.

Baturin, G.N., 1988. The Geochemistry of Manganese and Manganese Nodules in the Ocean. D. Reidel Publishing Company, Boston.

Beyer, C., Klemme, S., Wiedenbeck, M., Stracke, A., Vollmer, C., 2012. Fluorine in nominally fluorine-free mantle minerals: experimental partitioning of F between olivine, orthopyroxene and silicate melts with implications for magmatic processes. Earth Planet. Sci. Lett. 337–338, 1–9.

Bideau, D., Hebert, R., Hekinian, R., Cannat, M., 1991. Metamorphism of deep-seated rocks from the Garrett ultrafast transform (East Pacific Rise near 13-degrees-25'S). J. Geophys. Res. B, Solid Earth Planets 96 (B6), 10079–10099.

Bischoff, J.L., Dickson, F.W., 1975. Seawater-basalt interaction at 200 degrees C and 500 bars - implications for origin of sea-floor heavy-metal deposits and regulation of seawater chemistry. Earth Planet. Sci. Lett. 25 (3), 385–397.

Bostock, M.G., Hyndman, R.D., Rondenay, S., Peacock, S.M., 2002. An inverted continental Moho and serpentinization of the forearc mantle. Nature 417 (6888), 536–538.

Chavrit, D., et al., 2016. The contribution of hydrothermally altered ocean crust to the mantle halogen and noble gas cycles. Geochim. Cosmochim. Acta 183, 106–124.

Claret, F., et al., 2010. Natural iodine in a clay formation: implications for iodine fate in geological disposals. Geochim. Cosmochim. Acta 74 (1), 16–29.

Dalou, C.l., Koga, K., Shimizu, N., Boulon, J., Devidal, J.-L., 2012. Experimental determination of F and Cl partitioning between lherzolite and basaltic melt. Contrib. Mineral. Petrol. 163, 591–609.

Deer, W.A., Howie, R.A., Zussman, J., 1992. An Introduction to the Rock Forming Minerals. Longman Scientific and Technical. 696 pp.

Dick, H.J.B., Lin, J., Schouten, H., 2003. An ultraslow-spreading class of ocean ridge. Nature 426, 405–412.

Dick, H., et al., 2017. Expedition 360 summary. In: Proceedings of the International Discovery Program.

Dick, H.J.B., et al., 2000. A long in situ section of the lower oceanic crust: results of ODP Leg 176 drilling at the Southwest Indian Ridge. Earth Planet. Sci. Lett. 179, 31–51.

Expedition 309/312 Scientists, 2006. Site 1256. In: Teagle, D.A.H., et al. (Eds.), Proceedings IODP. Integrated Ocean Drilling Program Management International Inc., Washington DC, pp. 1–549.

Ito, E., Anderson, A.T. Jr., 1983. Submarine metamorphism of gabbros from the Mid-Cayman Rise: petrographic and mineralogic constraints on hydrothermal processes at slow-spreading ridges. Contrib. Mineral. Petrol. 82 (4), 371–388.

Ito, E., Harris, D.M., Anderson, A.T., 1983. Alteration of oceanic-crust and geologic cycling of chlorine and water. Geochim. Cosmochim. Acta 47 (9), 1613–1624.

Joachim, B., et al., 2015. Experimental partitioning of F and Cl between olivine, orthopyroxene and silicate melt at Earth's mantle conditions. Chem. Geol. 416, 65–78.

John, B.E., et al., 2004. Determining the cooling history of in situ lower oceanic crust—Atlantis Bank, SW Indian Ridge. Earth Planet. Sci. Lett. 222 (1), 145–160.

John, T., Scambelluri, M., Frische, M., Barnes, J.D., Bach, W., 2011. Dehydration of subducting serpentinite: implications for halogen mobility in subduction zones and the deep halogen cycle. Earth Planet. Sci. Lett. 308 (1–2), 65–76.

Kendrick, M.A., 2012. High precision Cl, Br and I determination in mineral standards using the noble gas method. Chem. Geol. 292–293, 116–126.

Kendrick, M.A., 2018. Halogens in seawater, marine sediments and the altered oceanic lithosphere. In: Harlov, D.E., Aranovich, L.Y. (Eds.), The Role of Halogens in Terrestrial and Extraterrestrial Processes. Springer International Publishing, pp. 591–648.

Kendrick, M.A., Arculus, R.J., Burnard, P., Honda, M., 2013a. Quantifying brine assimilation by submarine magmas: examples from the Galápagos Spreading Centre and Lau Basin. Geochim. Cosmochim. Acta 123, 150–165.

Kendrick, M.A., et al., 2013b. Subduction zone fluxes of halogens and noble gases in seafloor and forearc serpentinites. Earth Planet. Sci. Lett. 365, 86–96.

Kendrick, M.A., et al., 2014. Subduction-related halogens (Cl, Br and I) and H_2O in magmatic glasses from Southwest Pacific Backarc Basins. Earth Planet. Sci. Lett. 400, 165–176.

Kendrick, M.A., D'Andres, J., Holden, P., Ireland, T., 2018. Halogens (F, Cl, Br, I) in thirteen USGS, GSJ and NIST international rock powder and glass reference materials. Geostand. Geoanal. Res.

Kendrick, M.A., et al., 2017. Seawater cycled throughout Earth's mantle in partially serpentinized lithosphere. Nat. Geosci. 10, 222–228.

Kendrick, M.A., Honda, M., Vanko, D.A., 2015. Halogens and noble gases in Mathematician Ridge meta-gabbros, NE Pacific: implications for oceanic hydrothermal root zones and global volatile cycles. Contrib. Mineral. Petrol. 170 (5–6), 1–20.

Lu, Z.L., Jenkyns, H.C., Rickaby, R.E.M., 2010. Iodine to calcium ratios in marine carbonate as a paleo-redox proxy during oceanic anoxic events. Geology 38 (12), 1107–1110.

Macleod, C.J., et al., 2017. Expedition 360 methods.

Magenheim, A.J., Spivack, A.J., Michael, P.J., Gieskes, J.M., 1995. Chlorine stable isotope composition of the oceanic crust: implications for Earth's distribution of chlorine. Earth Planet. Sci. Lett. 131, 427–432.

Muramatsu, Y., et al., 2007. Halogen concentrations in pore waters and sediments of the Nankai Trough, Japan: implications for the origin of gas hydrates. Appl. Geochem. 22 (3), 534–556.

Natland, J.H., Dick, H.J.B., 2001. Formation of the lower ocean crust and the crystallization of gabbroic cumulates at a very slowly spreading ridge. J. Volcanol. Geotherm. Res. 110 (3–4), 191–233.

Nehlig, P., Juteau, T., 1988. Deep crustal seawater penetration and circulation at ocean ridges - evidence from the Oman ophiolite. Mar. Geol. 84 (3–4), 209–228.

Opdyke, B.N., Walter, L.M., Huston, T.J., 1993. Fluoride content of foraminiferal calcite: relations to life habitat, oxygen isotope composition, and minor element chemistry. Geology 21 (2), 169–172.

Pagé, L., Hattori, K., de Hoog, J.C.M., Okay, A.I., 2016. Halogen (F, Cl, Br, I) behaviour in subducting slabs: a study of lawsonite blueschists in western Turkey. Earth Planet. Sci. Lett. 442, 133–142.

Philippot, P., Agrinier, P., Scambelluri, M., 1998. Chlorine cycling during subduction of altered oceanic crust. Earth Planet. Sci. Lett. 161 (1–4), 33–44.

Price, N.B., Calvert, S.E., 1973. The geochemistry of iodine in oxidised and reduced recent marine sediments. Geochim. Cosmochim. Acta 37 (9), 2149–2158.

Reeves, E.P., et al., 2011. Geochemistry of hydrothermal fluids from the PACMANUS, Northeast Pual and Vienna Woods hydrothermal fields, Manus Basin, Papua New Guinea. Geochim. Cosmochim. Acta 75 (4), 1088–1123.

Rioux, M., Cheadle, M.J., John, B.E., Bowring, S.A., 2016. The temporal and spatial distribution of magmatism during lower crustal accretion at an ultraslow-spreading ridge: high-precision U–Pb zircon dating of ODP Holes 735B and 1105A, Atlantis Bank, Southwest Indian Ridge. Earth Planet. Sci. Lett. 449, 395–406.

Sajeev, K., Osanai, Y., Kon, Y., Itaya, T., 2009. Stability of pargasite during ultrahigh-temperature metamorphism: a consequence of titanium and REE partitioning? Am. Mineral. 94 (4), 535–545.

Sano, T., et al., 2008. Boron and chlorine contents of upper oceanic crust: basement samples from IODP Hole 1256D. Geochem. Geophys. Geosyst. 9 (12), Q12O15.

Seyfried, J.W.E., Berndt, M.E., Janecky, D.R., 1986. Chloride depletions and enrichments in hydrothermal fluids: constraints from experimental basalt alteration studies. Geochim. Cosmochim. Acta 50, 469–475.

Stakes, D., Mevel, C., Cannat, M., Chaput, T., 1991. Metamorphic stratigraphy of Hole 735B. In: Von Herzen, R.P., Robinson, P.T. (Eds.), Proceedings of the Ocean Drilling Program, Scientific Results. Ocean Drilling Program, pp. 153–180.

Straub, S.M., Layne, G.D., 2003. The systematics of chlorine, fluorine, and water in Izu arc front volcanic rocks: implications for volatile recycling in subduction zones. Geochim. Cosmochim. Acta 67 (21), 4179–4203.

Sun, W.D., et al., 2007. Chlorine in submarine volcanic glasses from the eastern Manus basin. Geochim. Cosmochim. Acta 71 (6), 1542–1552.

Vanko, D.A., Stakes, D., 1991. Fluids in oceanic layer 3: evidence from veined rocks, Hole 735B, Southwest Indian Ridge. In: Von Herzen, R.P., Robinson, P.T., et al. (Eds.), Proceedings of the Ocean Drilling Program, Scientific Results.

Webster, J.D., 1990. Partitioning of F between H_2O and CO_2 fluids and topaz rhyolite melt - implications for mineralising magmatic-hydrothermal fluids in F-rich granitic systems. Contrib. Mineral. Petrol. 104 (4), 424–438.

Zhang, C., Wang, L.-X., Marks, M.A.W., France, L., Koepke, J., 2017. Volatiles (CO_2, S, F, Cl, Br) in the dike-gabbro transition zone at IODP Hole 1256D: magmatic imprint versus hydrothermal influence at fast-spreading mid-ocean ridge. Chem. Geol.